Investigation of the Seismic Background Noise of Gravitational-Wave Detectors Using Spectral Methods.

Fenyvesi Edit and Barnaföldi Gergely Gábor

Wigner Research Centre for Physics

Email: fenyvesi.edit@wigner.hu, barnafoldi.gergely@wigner.hu

2023

Abstract

Gravitational waves (GWs) are propagating fluctuations of spacetime. The sources of these waves can be, for example, colliding and merging binary system of compact objects. These systems typically consist of black holes and neutron stars.

Gravitational waves are currently detected with large-scale interferometric gravitational-wave detectors. The seismic vibrations of the Earth also contribute to the measurement noise of these interferometers. The vibrations are coupled into the structures holding the mirrors (test masses) of the interferometers, causing the mirrors to move. The displacement noise of the mirrors can be significantly reduced by choosing the proper special suspensions. The monitoring of seismic vibrations with seismometers enables the characterization of the continuously present background noise by spectral methods. During the planning process, the seismic noise dampening ability of the suspension of the mirrors can be determined. As a result of the procedure, a transfer function characterizing the given suspension is obtained, which can be used to calculate the amplitude spectral density of mirror displacement noise caused by the seismic noise background measured at a given installation location.

Seismic vibrations, can also be detected with accelerometers and geophones in addition to seismometers. The three instrument types have different inherent noise, sensitivity and frequency range. In this laboratory exercise, the students get to know the operation of the measuring different instruments and compare their capabilities. They find out which one(s) are suitable for measuring the seismic background noise of a GW detector. They calculate the mirror displacement noise of a fictive GW detector installed thirty meters below the Earth's surface. During the course they determine what gravitational wave producing phenomena could be observed with this detector given the measured noise background.

Table of contents

Gravitational waves 3
Quantities used during the laboratory exercise 5
Quantities characterizing seismic vibrations 5
Quantities that characterize measuring instruments 6
Measurement of seismic vibrations 6
Güralp CMG-3T 7
Raspberry Pi Shake 4d 8
Software 9
Measurements 9
Determining the signal-to-noise ratio of footsteps 9
Investigation of the seismic background noise of the Eötvös-balance laboratory 11
References 13

Gravitational waves

Einstein's general theory of relativity is the most accurate description of the gravitational interaction, verified by various experiments. According to the theory, matter bends space-time, and the curvature of space-time determines the movement of matter. This relationship is expressed by Einstein's field equations. We consider the vacuum solutions of the linearized form of the Einstein equations written in the Lorentz gauge to be gravitational waves (GWs) [1] [2].

Sources of GWs include the merger of binary systems consisting of black holes and neutron stars [3]. Initially, the two compact celestial objects orbit around the common center of mass. A binary can consist of two black holes (BBH), or two neutron stars (BNS), or one neutron star and one black hole (BHNS). Through the emission of the GW, the total energy of the bound system decreases, therefore the distance between the celestial bodies decreases continuously, while the orbital frequency, and thus the frequency of the emitted wave increases. Finally, the members of the double merge, in the case of BBH and BHNS, they form a single black hole. In the BNS case, either another neutron star or a black hole is created. The generated GWs travel at the speed of light. When they reach the Earth, they cause the deviations of space-time from the local curvature. The relative distortion is of the order of 10^{-22} [4].

GWs are detected with giant-sized laser interferometers (Figure 1), which are improved versions of the original Michelson interferometers [4]. The parts of an interferometer are a laser, a beam splitter, two mirrors, and a photodetector. The beam splitter disunites the laser beam into two perpendicular beams. The mirrors at the end of the arms reflects the beams to the beam splitter, which recombinates them. Upon recombination, the beams interfere, and the intensity of the resulting light is measured by a photodetector. If the mirrors of the interferometer move relative to each other, the intensity of the light detected by the photodetector changes.

A GW passing the interferometer's arms causes change of the relative length, and thus the phase shift of the split beams relative to each other. If the length of the interferometer's arm is much smaller than the wavelength of the GW, the change in the length of the arm is proportional to the space-time perturbation caused by the wave. In order to be able to detect relative changes in the order of 10^{-22}, the laser light has to travel a few thousand km along the arms. The arms are 3-4 km long, so two mirrors must be placed near the beam splitter so that to reflect the laser beam reflected from the mirrors at the end of the arms three hundred times more (Fig 1).

The following GW observatories are currently operating on Earth: aLIGO is in the United States of America [5], adVirgo in Italy [6], KAGRA in Japan [7], and GEO600 in Germany [8]. LIGO-India is a planned advanced GW observatory to be located in India as part of the worldwide network of detectors [9]. Einstein Telescope [10][11][12] and Cosmic Explorer [13] are proposed third-generation ground-based GW detectors, while TianQin [14], Taiji [15], Deci-hertz Interferometer Gravitational wave Observatory (DECIGO) [16], and the Laser Interferometer Space Antenna (LISA) [17] are proposed space-borne GW observatories.

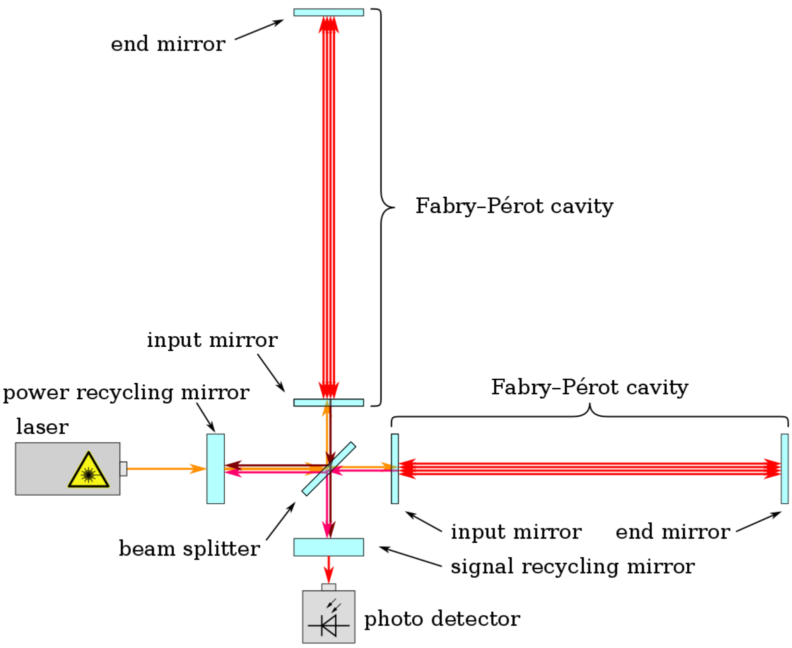

Fig 1. Schematic drawing of an interferometric GW detector [18].

The measurements of interferometers are affected by several noise components. One of these is seismic noise caused by the vibrations of the Earth. One of the tasks of the experiments is to identify and reduce these noises, since the vibrations cause unwanted displacements of the mirrors of the interferometers. The appropriate design of the suspension of the mirrors can mitigate the vibrations. By implementing the simplest suspension, the mirror and the suspension thread would form a pendulum. Based on what was described in [20], a better solution is to create a cascade consisting of several pendulums, in which the mass on the lowest pendulum is the mirror itself. Figure 2 shows how the suspension was implemented at the advanced Virgo GW detector in Italy. The total length of the suspension is 9 m.

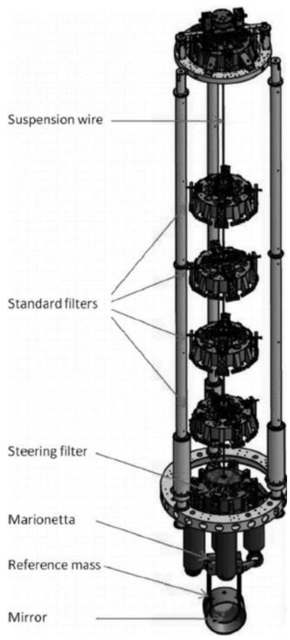

Fig 2. Suspension of test masses for the advanced Virgo gravitational-wave detector [19].

The seismic noise dampening ability of the suspension can be characterized by two transfer functions in the frequency domain. One characterizes the transmission of the vertical component of vibrations, and the other characterises the transmission of the horizontal component. If the amplitude spectral density of the horizontal (vertical) component of the seismic noise measured in the vicinity of the GW detector is multiplied by the horizontal (vertical) transfer function, we obtain the amplitude spectral density of the displacement noise caused by seismic vibrations.

The noise caused by seismic vibrations can be greatly reduced by installing GW detectors underground, as the vibrations are significantly attenuated in the by increasing the depth below the ground surface. A proposed subterranean GW detector is the European Einstein Telescope. Furthermore, the suspension of the Einstein Telescope's end-mirrors is planned to be implemented using the method used at adVirgo, but the total length of the suspension will be increased from 9 meters to 17 meters. Among the horizontal and vertical components of seismic noise, the horizontal one is dominant [20]. The purpose of this laboratory measurement is to qualify seismic noises using several methods.

Quantities used during the laboratory exercise

Quantities characterizing seismic vibrations

A seismic vibration with a frequency f, propagating in a given direction, at a given moment in time can be characterized by three quantities that can be calculated from each other: displacement, velocity, acceleration. If one of these is known, the other two can be calculated. If e.g. the acceleration a is known, the speed can be calculated from it: $v = \frac{a}{2\pi f}$, as well as the displacement: $d = \frac{v}{2\pi f} = \frac{a}{(2\pi f)^2}$.

Amplitude spectral density:

The different frequency components of seismic vibrations can be analyzed using spectral methods. Welch's periodogram method gives the amplitude spectral density (ASD) calculated from the given signal section using the Fourier spectrum of the vibrations [21]. The ASD shows the typical amplitude of the vibrations in a given period and at a given frequency. The ASD of seismic vibration acceleration is expressed in $\mathrm{m/s^2} Hz^{-1/2}$. By calculating the ASD values for a sufficient number of signal segments of the same length, it is possible to specify how often each amplitude level is taken up by the signal. The kth percentile belonging to a given frequency f informs us that in k percent of an examined period we can expect that the amplitude of the signal at the given frequency does not exceed the amplitude value belonging to the kth percentile. The fifth and ninety-fifth percentiles are usually given, as well as the median.

In order to characterize the seismic background noise of a given location with ASD percentiles, it is necessary to calculate the ASD values from a number of different signal segments in the order of hundreds. We would like to characterize the seismic background noise down to the 0.01 Hertz frequency range. In order to do this, the length of a given signal segment needs to be fixed in a few hundred seconds. Several hours of measurement data must be recorded and analyzed to collect the several hundred different segments.

The ratio of the signal amplitude to the standard deviation of the noise:

This quantity is useful if we want to identify and characterize phenomena that are limited to a short period and cause seismic vibrations. The signal can be given with any unit of measurement characteristic of the investigated phenomenon. If the statistical properties of the background noise change only slightly during the examined period, and the distribution of the amplitude of the noise approaches the normal distribution, the noise can be characterized by the standard deviation of the amplitude distribution (s). From time to time, short-term signal segments emerge from the noise, which are of interest to us. They are characterized by their maximum amplitude, A. The ratio of the amplitude of the outliers to the standard deviation of the noise (A/s) shows how much each outlier stands out from the noise.

Quantities that characterize measuring instruments

Frequency range: the instrument can detect signals with a frequency between the lower and upper limits of the frequency range.

The amplitude measurement range specifies the amplitude range of vibrations the measuring instrument can detect. The measuring instrument's self-noise limits the amplitude of vibrations the device can detect. This threshold is usually expressed with the ASD values of the self-noise. If we want to characterize the seismic background noise for example with the fifth and ninety-fifth percentiles, the measuring instrument must be chosen carefully. It may happen that the self-noise of the measuring instrument is so high that at least five percent of the time the background noise does not exceed the self-noise of the measuring instrument. In that case, the collected data characterize the measuring instrument's self-noise. The fifth percentiles calculated from the recorded data do not characterize the seismic noise background, but the measuring instrument's own noise. If we are lucky, there will be one of the higher percentile curves among the ones below the median, which only characterizes the noise background.

It may happen that the measuring device is affected by a vibration of such a high amplitude that it can no longer give an electrical signal proportional to the amplitude at its output. Then it emits the highest amplitude signal it can provide, and it saturates. If this happens often, the upper percentiles calculated from the signal may not show the real noise background.

Measurement of seismic vibrations

The instruments used in current laboratory excercise are designed to indicate and/or register earthquake waves by seismometers and the accelerometers (the latter is known as an accelerograph or strong motion seismometer). The seismometer converts ground movement into some other, more easily measurable physical quantity (e.g. electrical potential). The task of the seismometer is to detect the smallest possible ground movement. Today's modern devices are able to register ground displacement of the order of 10^{-5} mm. On the other hand, the task of the accelerometer is to record ground movements that occur during large earthquakes that can be sensed by humans and possibly cause damage.

A geophone is a device that converts the mechanical vibration of the ground into an electrical signal (Fig 3). The electric signal is generated by a strong permanent magnet moving inside a coil. Depending on the design, the moving element can be the magnet (less often) or the coil (usually), one is suspended on a sensitive spring, while the other is fixed to the geophone housing. The vibration of the moving element of the geophone is damped by short-circuiting the coil through the resistance R.

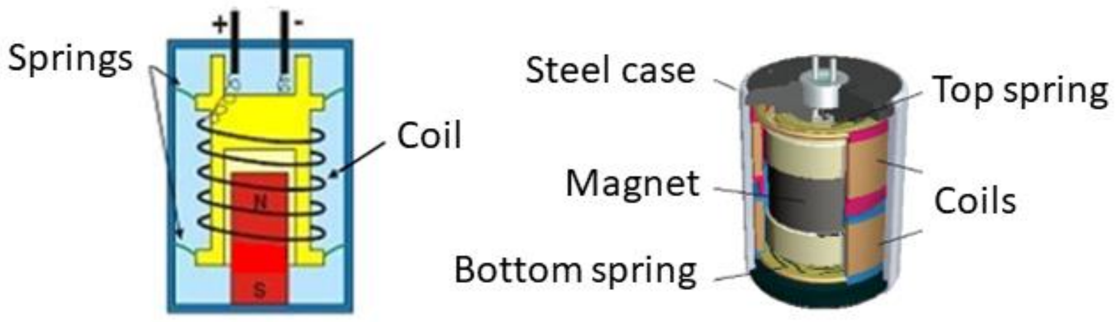

Fig 3. On the left is a schematic drawing of a geophone, and on the right is a drawing of a real geophone.

Güralp CMG-3T

The Güralp CMG-3T is a triaxial seismometer with a wide frequency range and low self-noise (Fig 4) [22]. More than 3,000 units of this type have already been installed worldwide.

The category of triaxial seismometers, to which the Güralp CMG-3T also belongs, transmits measurement data via three channels, providing mutually perpendicular vibration signals in the X, Y and Z directions. With correct settings, the three directions are N-S, E-W and vertical. The vibrations of the three directions are detected by three independent internal sensors.

In the sensor, the test mass is suspended so that it remains in one place, while the rest of the seismometer is attached to the ground to absorb its vibrations as much as possible. The sensors detect these displacements relative to the test masses.

Fig 4. Güralp CMG-3T seismometer

Raspberry Pi Shake 4d

Raspberry Shake 4D (RS4D) is a small device developed for the detection of seismic vibrations (Fig 5, Fig 6) [23]. Due to its low price, it is more accessible than a professional seismometer of higher sensitivity, wider frequency range and lower internal noise [24]. It is widely used for educational purposes, but it has also been shown to be applicable in some scientific experiments. Data collected by the volunteer-run Raspberry Shake monitoring network [25] are useful addition to the databases of seismic measurement data recorded by professional seismometers.

Three accelerometers are installed on the RS4D card, which can detect ground vibrations in three mutually perpendicular directions (N-S, E-W, vertical). A geophone is also connected to the card, which only measures in the vertical direction. The RS4D unit must be connected to a RaspberryPi board computer, which provides the power supply and control of the unit as well as the transmission of measurement data to the outside world.

Fig 5. Raspberry Shake 4D contains a geophone, the blue RS4D board with three accelerometers, connected to a green RaspberryPi board computer [17].

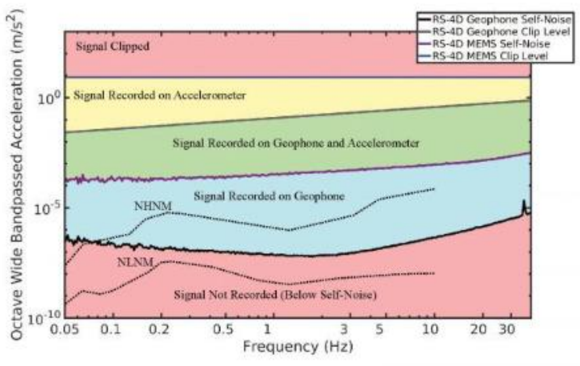

Fig 6. One can read the self-noise of the Raspberry Shake 4D sensors and their saturation level (specified by acceleration) as a function of frequency.

Software

We use python codes to process the measurement data. Data files from Güralp and Raspberry Shake are standard mseed files [26], which can be read, processed and analysed by using the python's obspy package [27]. Before the laboratory excercise, it is necessary to install the Anaconda python distribution [28]. In addition, a development environment must be installed, PyCharm is recommended [29]. Students have to install the obspy package, but the other necessary packages are already included in Anaconda. All the programs needed to perform the tasks of the laboratory can be found in the Seismo folder:

https://mycloud.wigner.hu/apps/files/?dir=/Gyakorlat/Seismo&fileid=1732827

The development environment is required to run and modify them. The codes have to be modified manually as described in the tasks given below.

Measurements

One goal of the measurements is to compare the abilities of the Güralp CMG-3T and the Raspberry Shake 4D instruments at the KFKI campus (Csillebérc, Hungary) in the Vesztergombi High-energy Laboratory (VLAB) Jánossy Underground Research Laboratory [30]. On one hand, we would like to find out with what signal-to-noise ratio (SNR) our measuring devices are able to detect steps, and rank them according to their SNR.

On the other hand, we would like to know whether the Raspberry Shake 4D can measure the seismic background noise in the underground laboratory. To answer this question, we use noise spectra calculated from the Güralp seismometer's signal as a reference, with a well-known self-noise.

Finally, from the displacement ASD values of seismic background noise measured by Güralp, we determine the mirror displacement noise of an fictive GW detector of the same design as the Einstein Telescope, installed 30 meters below the ground at KFKI campus. The resulting mirror displacement noise is compared with the maximum displacement noise allowed for ET and adVirgo.

Determining the signal-to-noise ratio of footsteps

1. The necessary measurements are performed in the Jánossy Underground Research Laboratory, in the Eötvös-inga laboratory, at the level -3. During the measurement, make sure not to disturb the Eötvös pendulum in the laboratory or move its wires! After we arrive at the laboratory, we record the data necessary to compute the measurement noise. Instruments record data continuously, so we only have to do the following: after entering the lab., everyone should stand still for half a minute, but record the start and end time of the this recording. Then one person should walk from the entrance of the laboratory to the far end, stand still for a few seconds, then go back to the entrance. Meanwhile, this

person has to count his/her steps forward and backward, too. The others stand still during this time in order not to disturb the measurement. Make a video recording of the measurement and write down the following data:

- start time of noise measurement
- end time of noise measurement
- number of steps from the entrance to the end of the laboratory
- number of steps from the end of the laboratory to the entrance

2. After returning to the office where data is analyzed, calculate the measurement noise of the following channels: Güralp vetical, Shake's geophone, and Shake's vertical accelerometer!

   The leader of the laboratory excercise downloads the necessary data files. The data files should be read using the **read(filename, start, end)** function of the **noise.py** program. The function returns with two figures. One of them shows the raw data set. We can check the data with our eyes, and if we see that not only the measurement noise was included in the selected data series, but also outliers are visible, change the start and end parameters and run the program again and again until only measurement noise remains (as long section of it as possible). The function also shows the data recorded between the start and end times on a histogram. The standard deviation that characterizes the noise can be read from this figure. Save the resulting graphs and copy them into the measurement documentation.

   Perform this procedure for each of the following channels:

   - Güralp's vertical channel
   - Shake's geophone
   - Shake's vertical accelerometer

3. The steps are analyzed with the **footsteps.py** program. The same files must be read in as in the previous point, but this time the data sections containing the steps must be searched. The **steps(filename, start, end, noise_std)** function finds each step and marks them on the plot showing the data. It determines the signal-to-noise ratio from the maximum of the signal of the steps and displays the obtained values on the plot.

   Let's make a figure showing the footsteps with the python program's **steps()** function. The function requires the following argument: **noise_std** value characterizing the standard deviation of the measurement noise, obtained previously.

   Create the diagrams showing the steps for each of the following channels:

   - Güralp's vertical channel
   - Shake's geophone
   - Shake's vertical accelerometer

   Based on the obtained signal-to-noise ratios, rank the three measuring devices according to their step detection ability, from best to worst.

Use the figures to answer the following questions:

- Can we find any signal sections where the signal became saturated as a result of the step? With which devices can this phenomenon be observed?
- Can we find a step that one instrument could detect, but an other could not?

Investigation of the seismic background noise of the Eötvös-balance laboratory

Our goal is to find out whether the instruments of Raspberry Shake 4D can measure the seismic background noise in the shaft. The quantities to analyze are the median and fifth and ninety-fifth percentiles of the displacement ASD values (at a given frequency) calculated from the data of the given measuring device. The Güralp's self-noise is so low that we can assume that the displacement ASD measured by the instrument in the shaft characterizes the real noise background and not the device's self-noise. Therefore, in the following, the displacement ASD values measured by Güralp in a quiet period along the three directions (N-S, E-W, and vertical) will be used as a reference.

4. From the data of Güralp, determine the three reference displacement ASD curves (both median and percentiles) for a quieter period in the underground laboratory. It is recommended to choose a weekend night. Let's compare the background noise with Shake 4D's instruments' sensitivity thresholds published in the literature. For this purpose, let's run the **ref_background.py** program. We get three different figures according to the three directions (N-S, E-W and vertical). The figure for the vertical direction shows the displacement noise of Güralp, the self-noise of Shake's geophone, and the self-noise of the vertical accelerometer.

   Let's compare the Güralp's graph with the self-noise graphs of the other two devices. One can determine whether any of them would be able to measure the reference displacement noise calculated from the vertical component of the background noise in the laboratory (including median and percentiles). In the case of the two horizontal directions, we can only compare the data of the Güralp and the accelerometers.

5. Compute the displacement ASD graphs (median and 5th and 95th percentiles) from the measurement data of different channels of Shake corresponding to the time period investigated in the previous section. After running the program, we get four figures:
   - on the first one, we can see the geophone's displacement ASD graph together with the self-noise noise reported on the data sheet of the device, and the Güralp's displacement ASD curves corresponding to the vertical direction.
   - on the second one, we can see the vertical accelerometer's displacement ASD graph together with the self-noise noise reported on the data sheet of the device, and the Güralp's displacement ASD curves corresponding to the vertical direction
   - on the third one, we can see the E-W accelerometer's displacement ASD graph together with the self-noise noise reported on the data sheet of the device, and the Güralp's displacement ASD curves corresponding to the E-W direction.

- on the third one, we can see the S-N accelerometer's displacement ASD graph together with the self-noise noise reported on the data sheet of the device, and the Güralp's displacement ASD curves corresponding to the S-N direction.

Let's examine the four figures above one by one and decide whether the Shake's devices detect the given component of the seismic background noise, or they provided data resulting from their self-noise.

6. With the help of the **Einstein_telescope.py** program, let's examine what would be the mirror displacement noise of a GW detector similar to ET, installed under the KFKI campus.

   A transfer function characterizes the seismic noise damping ability of the suspension of ET's end mirrors in the horizontal direction. The horizontal component of the seismic noise is represented by the median of the horizontal displacement ASD values computed from the measurement data of Güralp. The program does the following: for each f frequencies, it multiplies the median ASD value with the transfer function's value of the given frequency.

   It performs this for all f values of the examined frequency range.

   Finally, the program provides a diagram showing the following curves:

   - the ASD plot of the mirror displacement noise of the fictive detector
   - ASD graph of the allowed maximum mirror displacement noise of ET
   - ASD graph of the mirror displacement noise measured at the adVirgo detector

   Compare the three graphs and decide whether our fictive detector comply with the design requirements of ET.

   After this, let's run the **binaries.py** program. The resulting figure shows the detectability threshold of GW signals from various sources. Which of the GW detectors can detect the different types of signals? Based on the figure, let's summarize what would be the advantages of the underground construction of a GW detector from the point of wiev of the detectability of signals?

References

[1] A. Einstein, Näherungsweise Integration der Feldgleichungen der Gravitation.,Sitzungber. Preuss. Akad. Wiss. Berlin, part 1, p. 688, 1916.

[2] A. Einstein, Über Gravitationswellen, Sitzungber. Preuss. Akad. Wiss. Berlin, part 1, p. 154, 1918.

[3] LIGO-Virgo Compact Binary Catalogue, https://catalog.cardiffgravity.org/

[4] Peter R Saulson, Fundamentals of Interferometric Gravitational Wave Detectors (2nd edition). WORLD SCIENTIFIC, April 2017

[5] https://www.ligo.caltech.edu/page/about-aligo

[6] http://public.virgo-gw.eu/advanced-virgo/

[7] https://gwcenter.icrr.u-tokyo.ac.jp/en/

[8] https://www.geo600.org/

[9] https://www.ligo-india.in/

[10] E.T. Scientific Committee, ET Design Report Update 2020, 2020.

[11] https://www.et-gw.eu/

[12] http://einsteinteleszkop.hu/hu

[13] https://cosmicexplorer.org/

[14] https://en.wikipedia.org/wiki/TianQin

[15] https://en.wikipedia.org/wiki/Taiji_Program_in_Space

[16] http://tamago.mtk.nao.ac.jp/spacetime/decigo_e.html

[17] https://www.elisascience.org/

[18] https://commons.wikimedia.org/wiki/File:LIGO_simplified.svg

[19] T. Accadia et al., A state observer for the Virgo inverted pendulum, The Review of Scientific Instruments 82(9), p. 094502, 2011.

[20] L. Trozzo, F. Badaracco; Seismic and Newtonian Noise in the GW Detectors, Galaxies 10, p. 20, 2022.

[21] P. D. Welch, The use of Fast Fourier Transform for the estimation of power spectra: A method based on time averaging over short, modified periodograms, IEEE Transactions on Audio and Electroacoustics, AU-15 (2), p. 70–73.

[22] https://www.guralp.com › DAS-030-0001

[23] https://raspberryshake.org/

[24] R. E. Anthony et al., Do Low-Cost Seismographs Perform Well Enough for Your Network? An Overview of Laboratory Tests and Field Observations of the OSOP Raspberry Shake 4D, Seismological Research Letters 90 (1), p. 219–228, 2019.

[25] https://raspberryshake.org/data-center/

[26] https://docs.obspy.org/packages/obspy.io.mseed.html

[27] https://docs.obspy.org/

[28] https://www.anaconda.com/products/distribution

[29] https://www.jetbrains.com/pycharm/

[30] https://vlab.wigner.hu/